A NEW CONVECTIVE ADJUSTMENT SCHEME AND ITS IMPACT ON THE ECMWF MODEL

M.J. Miller
European Centre for Medium Range Weather Forecasts
Reading, U.K.

Abstract

This paper is intended to introduce a new convective parameterization scheme for use in numerical weather prediction models, and which may have equal applicability to climate and possibly mesoscale models although this has yet to be well demonstrated. Since the original basis for the scheme and its design and testing is already documented by Betts and Miller, 1984, this paper will concentrate on conveying a basic understanding of the convection scheme and demonstrating the scheme's performance in the ECMWF global forecast model.

1. INTRODUCTION

There are relatively few basic convective parameterization schemes in use, although each and every model seems to have a variant of these basic ideas. Each scheme has advantages and disadvantages, proponents and opponents, and all use rather simple (or trivial) cloud models to redistribute heat and moisture in the vertical. It is inevitable that the sophistication and increasing complexity of these cloud models is seen as the way to progress, particularly as observational studies identify important additional cloud physical and mesoscale processes such as anvil rainfall, mesoscale downdraughts, melting layers, etc. This 'phenomenological' approach to parameterization, of parameterizing each physical process and hoping that the components combine effectively is fraught with difficulty, and despite steady progress, model simulations can still generate unrealistic thermodynamic structures which inevitably impair model performance.

2. PHILOSOPHY

The convective adjustment scheme follows a different philosophy in that rather than representing the individual contributing physical processes, the scheme's primary objective is to ensure that the local vertical temperature and moisture structure, which in nature are strongly constrained in the presence of convection, remain realistic.

The concept of a quasi-equilibrium between the convective clouds and the larger-scale forcing is now well-established following earlier ideas of Ludlam (1980) and more recently by Arakawa and Schubert (1974), Lord and Arakawa (1982) and Lord (1982) and for shallow clouds, Betts (1973). This concept implies that convective regions have characteristic temperature and moisture structures which can be documented observationally as a basis for a convective adjustment procedure; several examples are discussed in Betts and Miller (1984). The moist adiabatic adjustment scheme (Manabe, 1965) is a special case of the deep part of the scheme to be described and is particularly limited by the fact that a saturated moist adiabat is not observed as a possible quasi-equilibrium state.

In the case of shallow convection, the fluxes due to the shallow clouds are normally such as to counter the drying and warming due to large-scale sinking motion. If these fluxes are not parameterized, the boundary layer structure typical of, for example, the trade-wind areas, will be distorted with the inversion descending to very near the surface, leading to an underestimation of the simulated surface fluxes. This deficiency was pointed out by Tiedtke (1981) and the ECMWF boundary layer scheme has recently been suitably enhanced to parameterize these fluxes (Tiedtke, 1983).

3. THE SCHEME

The scheme simultaneously adjusts the temperature (T) and moisture (q) profiles towards quasi-equilibrium 'reference' profiles for both deep, precipitating and shallow non-precipitating convection hence

$$\left(\frac{\partial \phi}{\partial t}\right)_{\text{convection}} = \frac{(\phi_R - \phi)}{\tau} \qquad (1)$$

where $\phi_R(p)$ is a reference profile for T or q and ϕ is the gridpoint value; τ is an 'adjustment' or 'relaxation' timescale. Both deep and shallow schemes hence require a choice of τ and computation at each convective gridpoint of ϕ_R.

The scheme is best explained with the aid of a flow chart, Fig. 1. The large-scale advective, radiation and surface fluxes modify the thermodynamic structure; this profile is then checked for conditional instability and cloud top found using a moist adiabat through a low level ϕ_E. Cloudtop height initially distinguishes shallow from deep convection (currently chosen around 750 mb in the forecast model).

Different reference profiles are constructed for deep and shallow convection with different integral constraints. The convective adjustment, defined by (1), then implicitly redistributes the heat and moisture. If the deep scheme is selected by cloud top but is found to give negative precipitation (because of weak subsidence for example), then the deep adjustment is not applied.

Instead, a shallow cloudtop is specified and the shallow adjustment made. For shallow convection the reference profile is constructed to satisfy the two separate constraints

$$\int_{P_B}^{P_T} C_p (T_R - T)dp = \int_{P_B}^{P_T} L (q_R - q)dp = 0 \qquad (2)$$

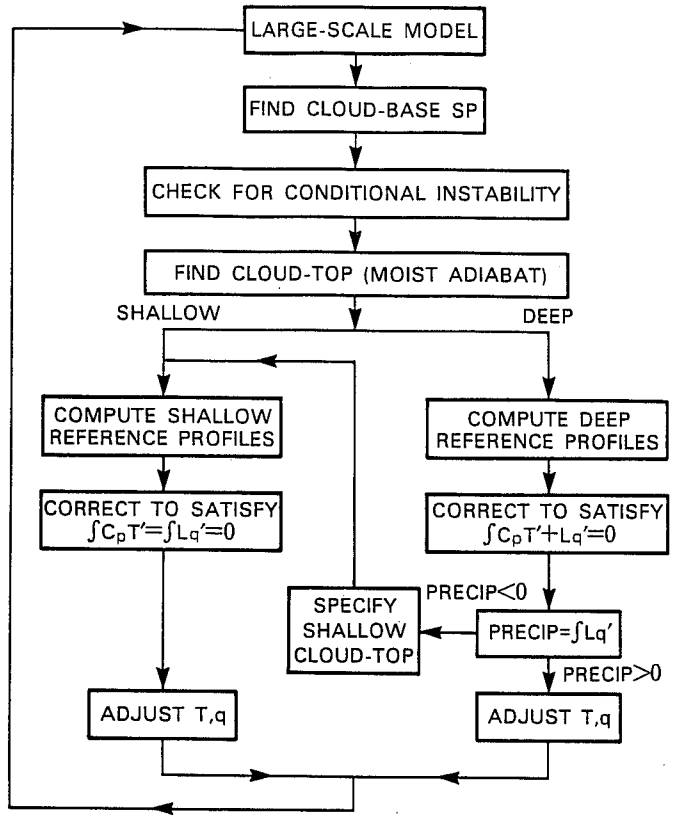

Fig. 1 Flowchart of convection scheme

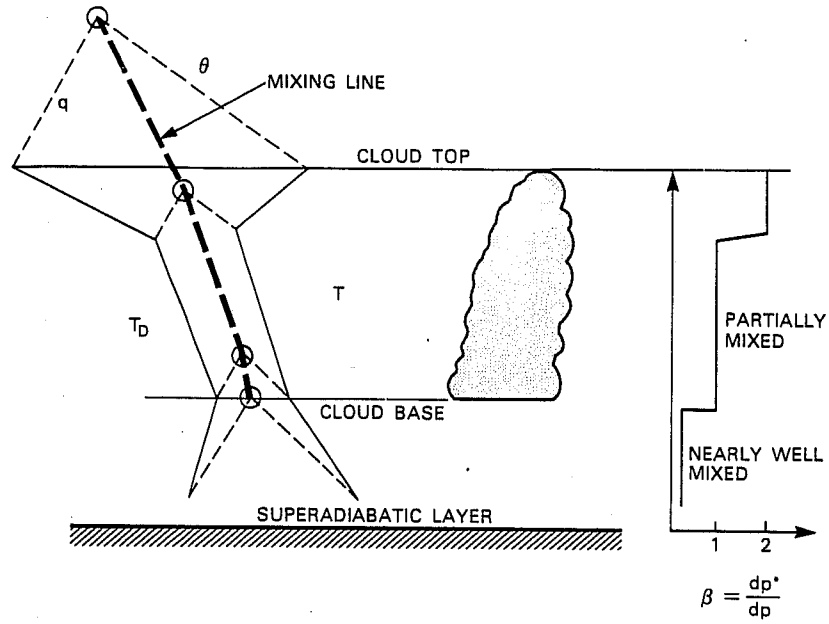

Fig. 2 Idealised cloudy boundary layer thermodynamic structure showing relationship between mixing line, temperature and dewpoint soundings and the parameter β = dp*/dp (see text).

where P_B, P_T are a cloudbase and cloudtop, respectively. These ensure that the net condensation rate is zero.

The deep scheme must satisfy the total enthalpy constraint

$$\int_{P_L}^{P_T} \left\{(C_pT + Lq)_R - (C_pT + Lq)\right\} dp = 0 \qquad (3)$$

where P_L is now a low level pressure (not the surface). The precipitation rate is then given by

$$PR = \int_{P_L}^{P_T} \frac{(q-q_R)}{\tau} \frac{dp}{g}$$

No liquid water is stored in the present scheme.

3.1 Reference thermodynamic profiles

a) Shallow convection reference profile

The shallow convection scheme is based on a parametric idealization of the coupling of a temperature and dewpoint structure of a convective layer to a mixing line (Fig. 2). Saturation level pressure $p^*(p)$ locates $\theta(p)$, $q(p)$ on this mixing line. Defining a parameter

$$\beta = \frac{dp^*}{dp}$$

then gives

$$\frac{\partial\theta}{dp} = \beta \left(\frac{\partial\theta}{\partial p^*}\right)_m$$

$$\frac{\partial q}{\partial p} = \beta \left(\frac{\partial q}{\partial p^*}\right)_m$$

where the suffix m denotes the mixing line. These equations relate the mean vertical profiles of θ and q to the gradient of the mixing line. The parameter β represents in some sense the intensity of mixing within and between convective layers.

The mixing line slope is computed from the saturation points of air at the level above the surface (representative of cloud-base properties) and the level above cloud top. The adjustment scheme is not applied below cloud-base (a dry diffusion scheme generates a mixed layer). A constant value of β is specified from cloud-base to the level just below cloud-top. A value of $\beta = 0.8$ is used. For the stable layer at cloud-top a value of β (typically ~2) is estimated internally from the gradients of p* across cloud-top.

A guess value of $\mathcal{P} = p^*-p$ is assumed at cloud-base, and first guess reference profiles are computed from β and the mixing line slope. Corrections ΔT, Δq (independent of pressure) are applied to the reference profiles to ensure the energy constraints are satisfied.

b) Deep convection reference profiles

The deep convection reference profiles are more empirically based. A temperature profile with a minimum in θ_{ES} at the freezing level is specified, so that the thermal structure is unstable to the moist adiabat in the lower troposphere and stable above. This is consistent with observations (Betts and Miller, 1984). Since there is only one energy constraint, it is necessary to specify more detail in the $\mathcal{P}$ structure (related to subsaturation) than for shallow convection. $\mathcal{P}$ is specified at three levels: a low level, the freezing level, and cloud-top with linear gradients in between. This is roughly equivalent to specifying a relative humidity structure. The instability below the freezing level is formulated in terms of the slope of the θ_{ESV} isopleth (Betts, 1983). It is computationally more economic to reinterpret this slope in terms of θ using

$$\frac{\partial\theta}{\partial p} = 0.85 \left(\frac{\partial\theta}{\partial p}\right)_{\theta_{ES}} \approx 0.95 \left(\frac{\partial\theta}{\partial p}\right)_{\theta_{ESV}}.$$

In the upper troposphere, the θ profile returns to θ_{ES} at cloudtop by interpolating the difference from the moist adiabat linearly with pressure. At present the energy corrections to the profiles required to satisfy (2) and (3) are assumed constant with height and only one iteration is required for good energy conservation.

4. SINGLE-COLUMN TESTS

The deep and shallow components of the scheme were developed, tested and tuned using a series of single column data sets: a GATE-wave data set (from Thompson et al., 1979) for deep convection, and BOMEX and ATEX datasets (Holland and Rasmusson, 1973; Augstein et al., 1973; Wagner, 1975) for shallow convection. A fourth dataset for an Arctic air-mass transformation (Okland, 1976) was used to test both schemes for conditions of strong surface fluxes. Details are in Betts and Miller (1984) and only selected results will be shown here.

Figs. 3, 4 and 5 illustrate the ability of the deep scheme to reproduce the diagnosed convective heating and drying for the GATE-wave data. The single-column model is provided with the large-scale forcing and surface flux terms and the convection scheme responds accordingly. Clearly the scheme performs very well indeed, although without a parameterization of a storage term the scheme cannot reproduce the lag in the precipitation cycle, Fig. 6. These results reflect, in part, the quasi-equilibrium behaviour of the dataset; nevertheless, similar tests with the Kuo (Kuo, 1965, 1974) and Arakawa-Schubert (Arakawa and Schubert, 1974) schemes do not give such good results.

As discussed earlier, the shallow scheme must represent the fluxes which maintain, for example, the trade wind inversion against subsidence. Figs. 7

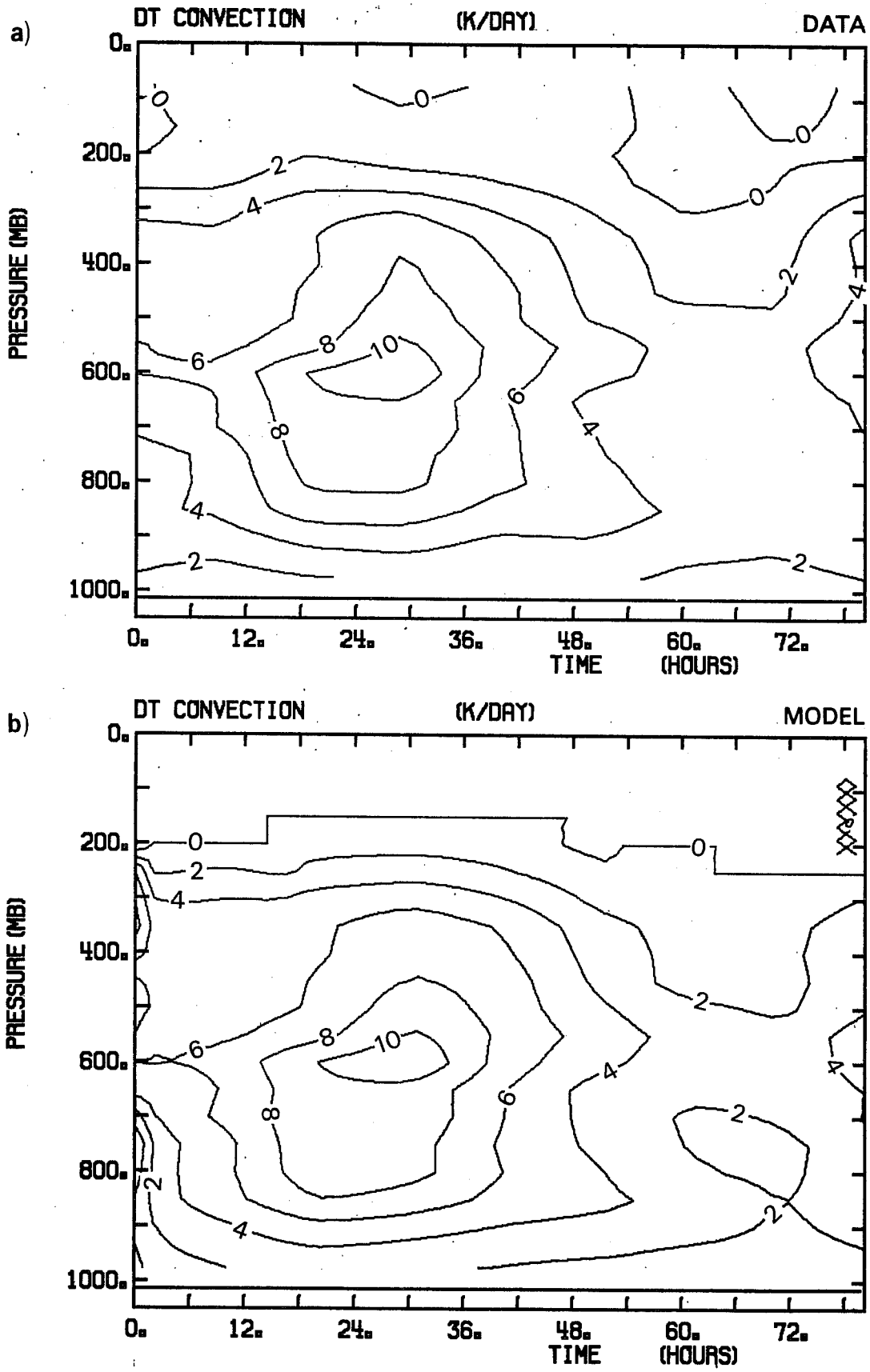

Fig. 3 Comparison of a) diagnosed and b) computed convective heating for GATE-wave data.

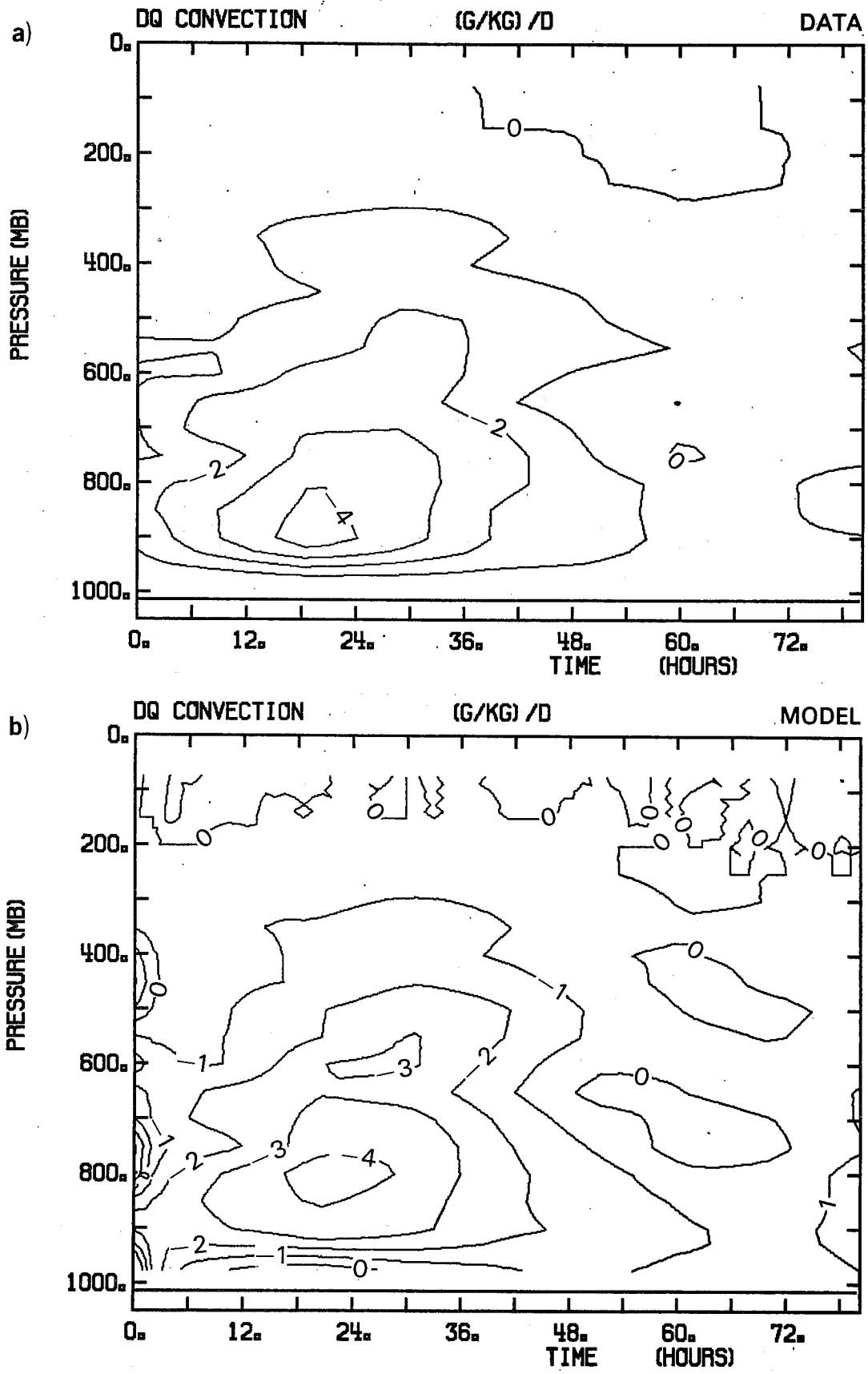

Fig. 4 As Fig. 3 for convective drying.

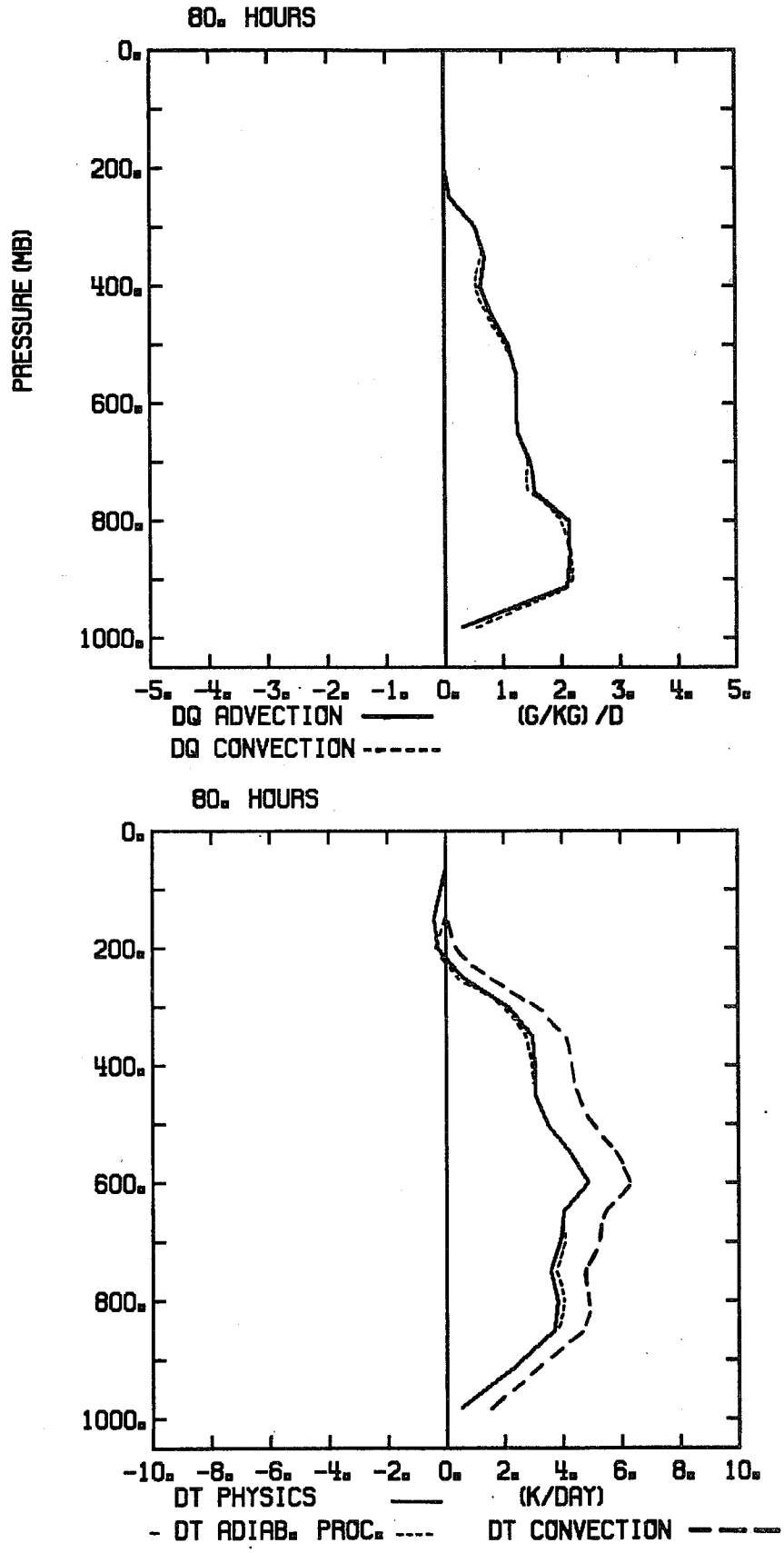

Fig. 5 80 hr mean vertical structure of prescribed adiabatic forcing terms and parameterized drying and heating for GATE-wave data due to convective and surface fluxes.

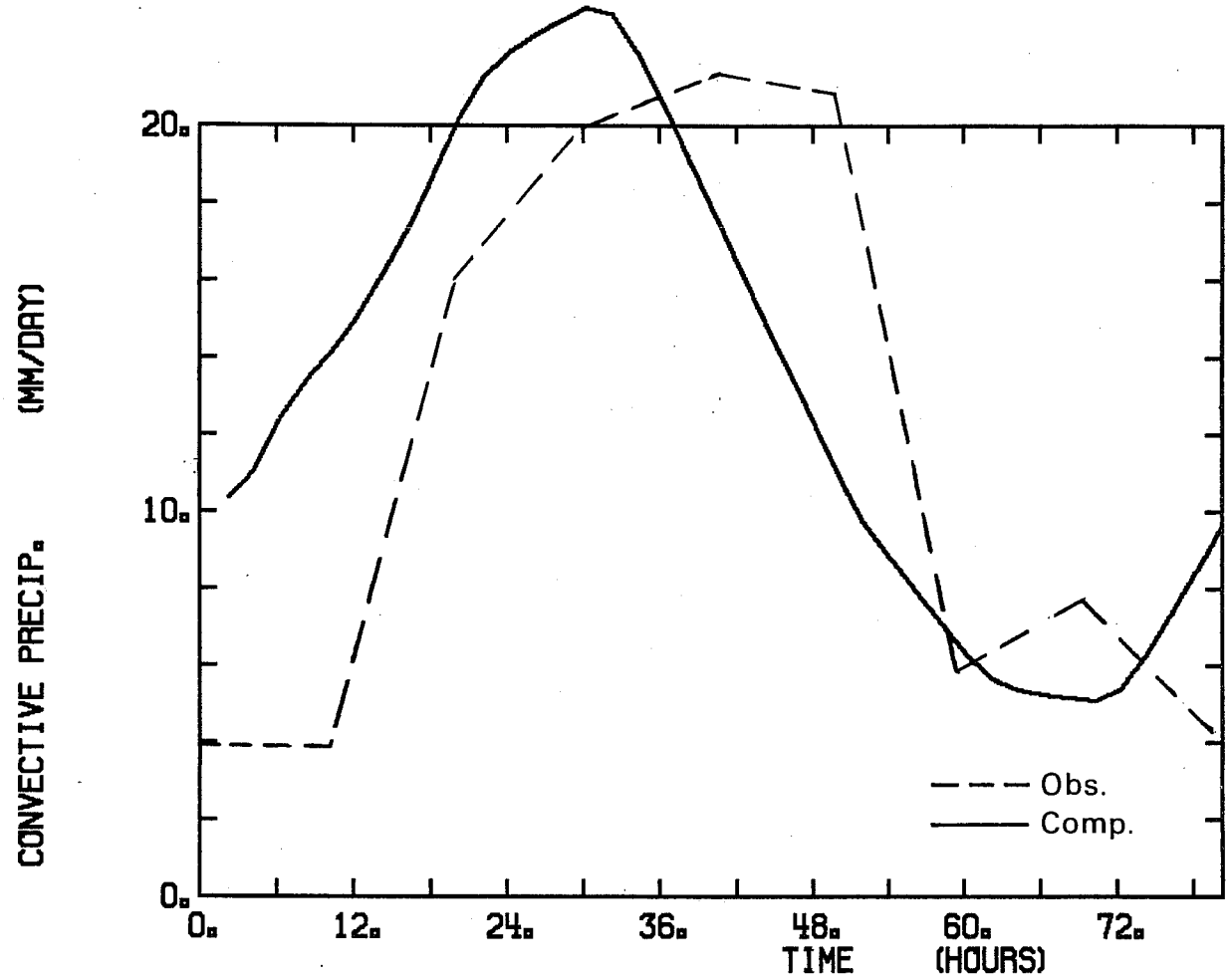

Fig. 6 Comparison of observed and computed rainfall.

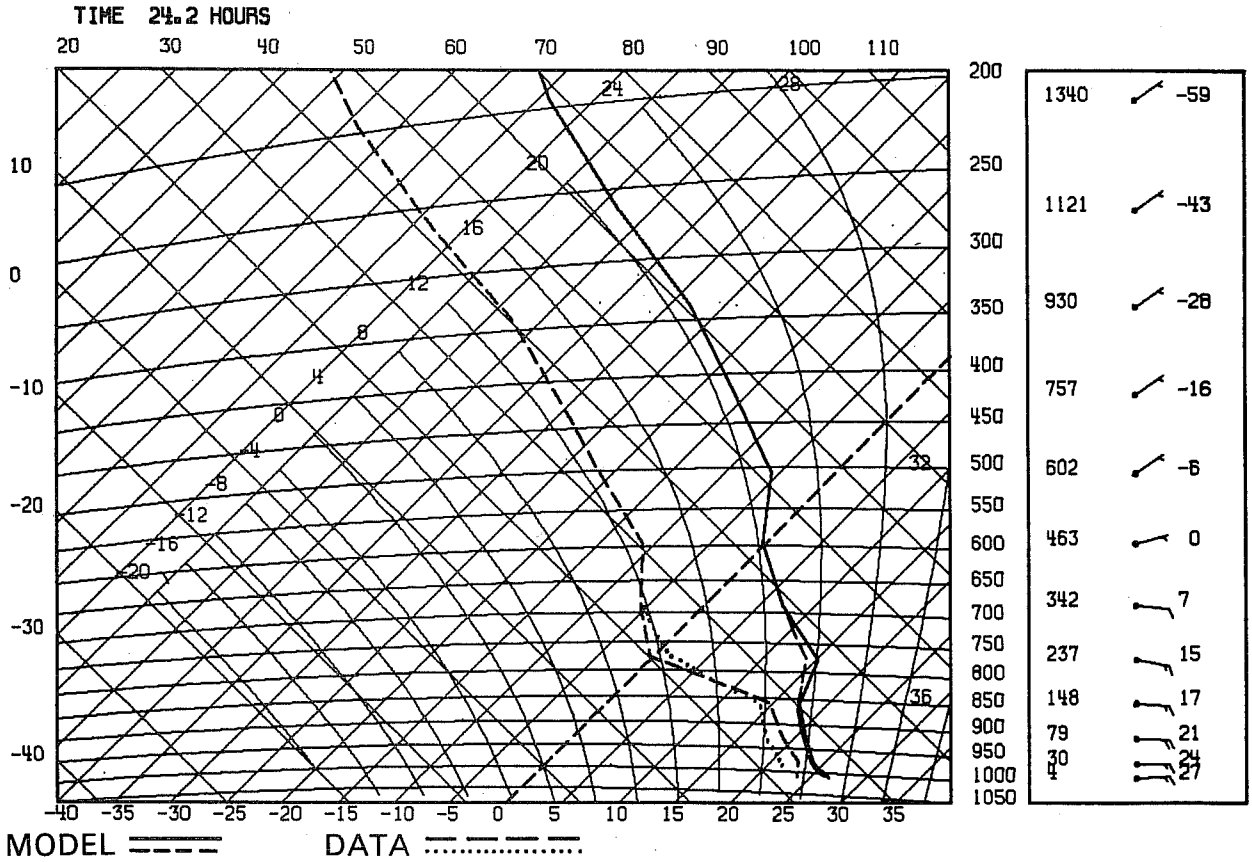

Fig. 7 Comparison of observed and model boundary layer structure for BOMEX

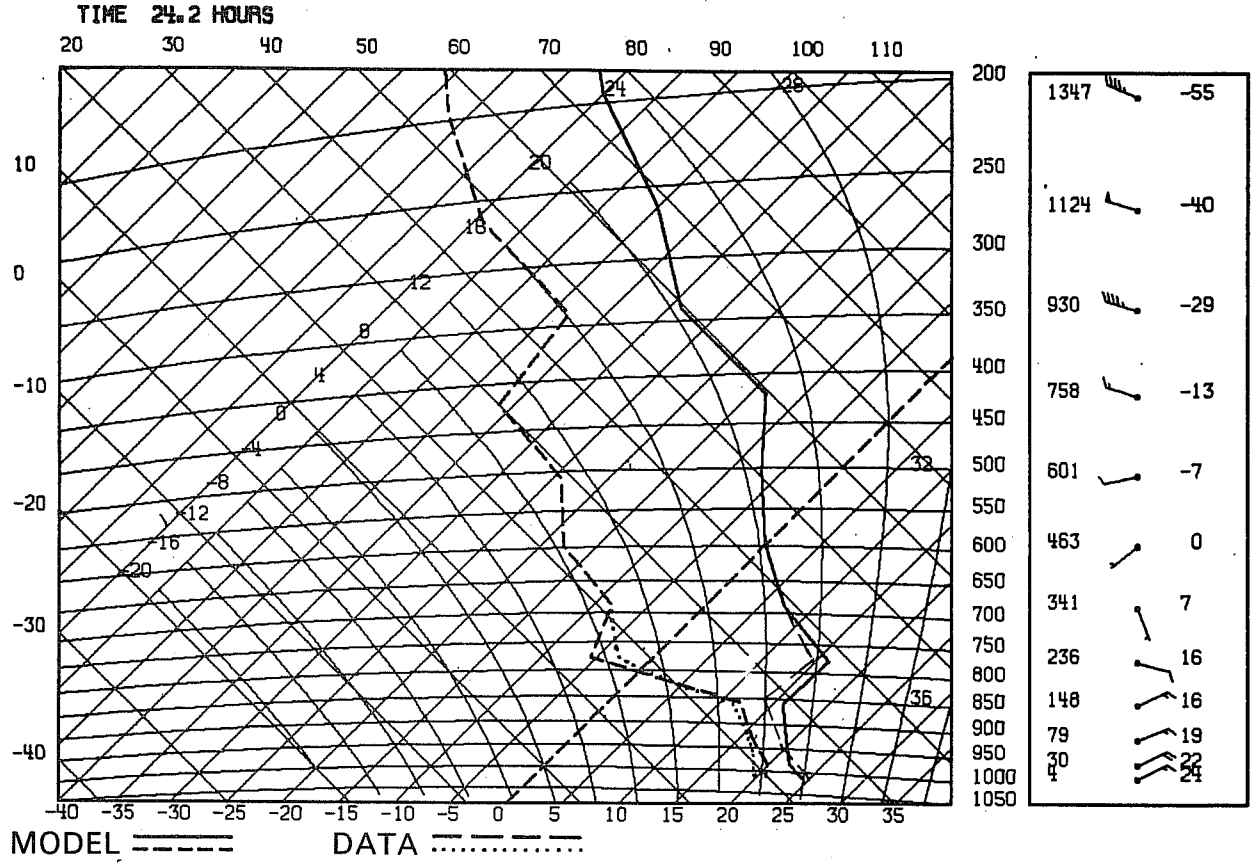

Fig. 8 As Fig. 7 for ATEX comparison.

and 8 show this is indeed the case for 24 hr tests using the BOMEX and ATEX data in a similar manner to the GATE data.

5. GLOBAL FORECASTS

Several 10-day forecasts at T63 spectral resolution have been carried out in which the operational KUO scheme and the shallow convection scheme were replaced by the new adjustment schemes. A longer integration (50 day T63) was also carried out. The following sections discuss these forecasts in terms of various indicators of model skill and consider the impact on the simulated flow.

5.1 Forecast 'skill'

For an ideal evaluation of forecast skill each forecast should be initialized from a data assimilation and analysis which uses the same model convection schemes in order to avoid initial imbalances and inconsistencies. To do this for a series of forecasts is a lengthy business and was only done for one case here, for which the reanalysed case performed slightly better.

Fig. 9 shows the mean skill scores for four T63 10 day forecasts evaluated using the anomaly correlations of height and temperature averaged over the Northern Hemisphere troposphere (1000-200 mb; 20°-80°N). Improvement is apparent by day 4 and increases steadily through the forecast period particularly in the height field. Other experiments not discussed here confirm this significant improvement, with rather larger improvement in the Northern Hemisphere winter half year compared to the summer half, when one or two forecasts show no improvement at all. A full appreciation of these forecast results and their synoptic impact is a major research undertaking with no simple answers, but this work will be attempted.

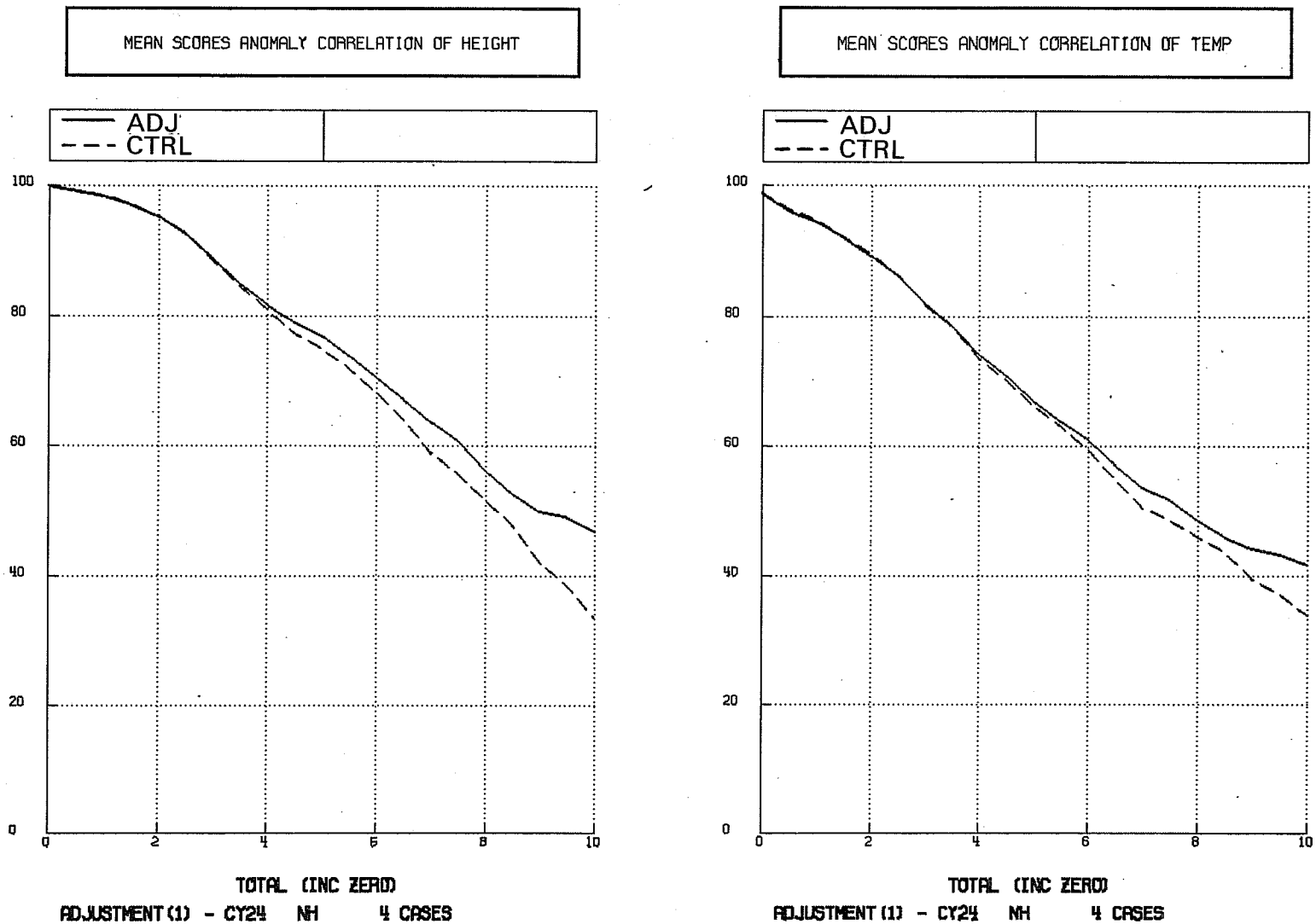

Fig. 9 Anomaly correlations for height and temperature averaged over 1000-200 mb and 20-82.5°N. Mean of four T63 forecasts.

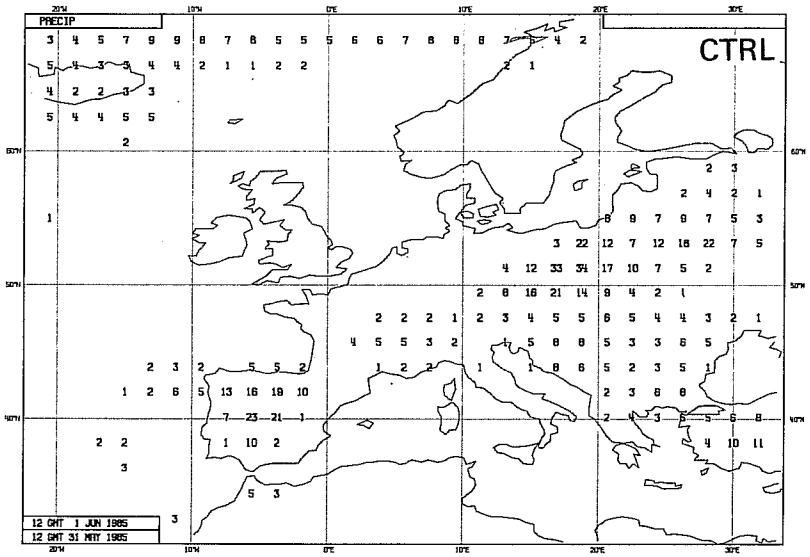

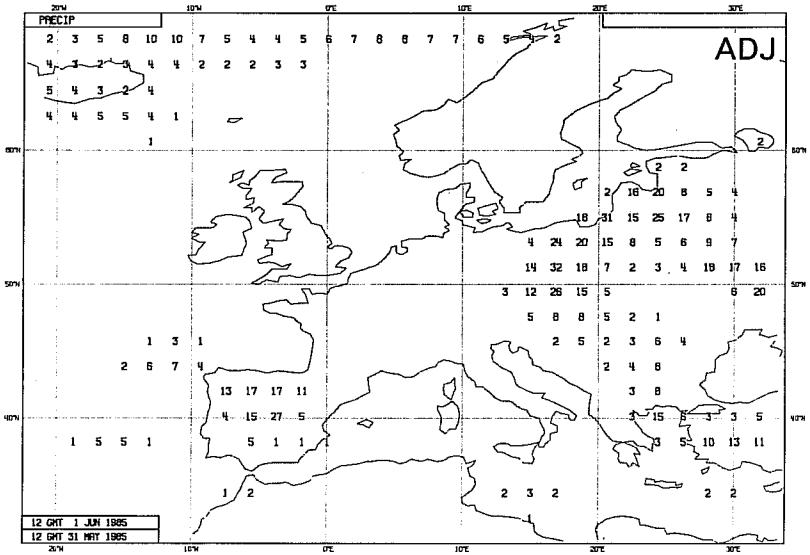

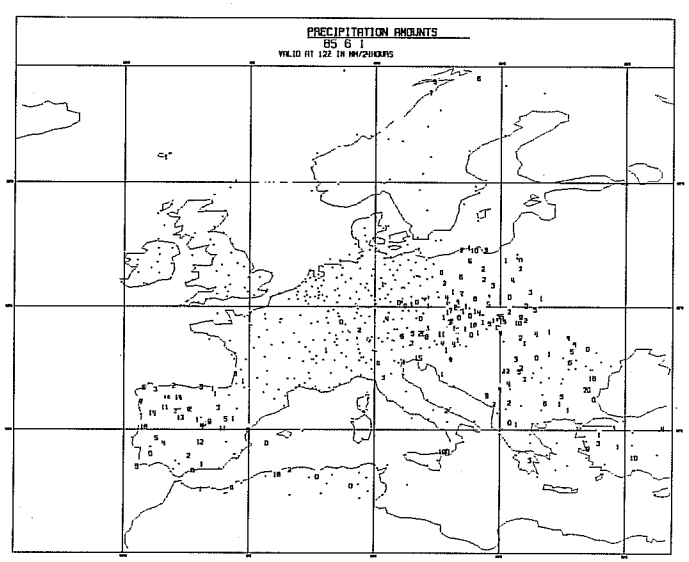

Fig. 10 Verification of 24 hr accumulated rainfall for day 2 of a T63 forecast and the control forecast against station data.

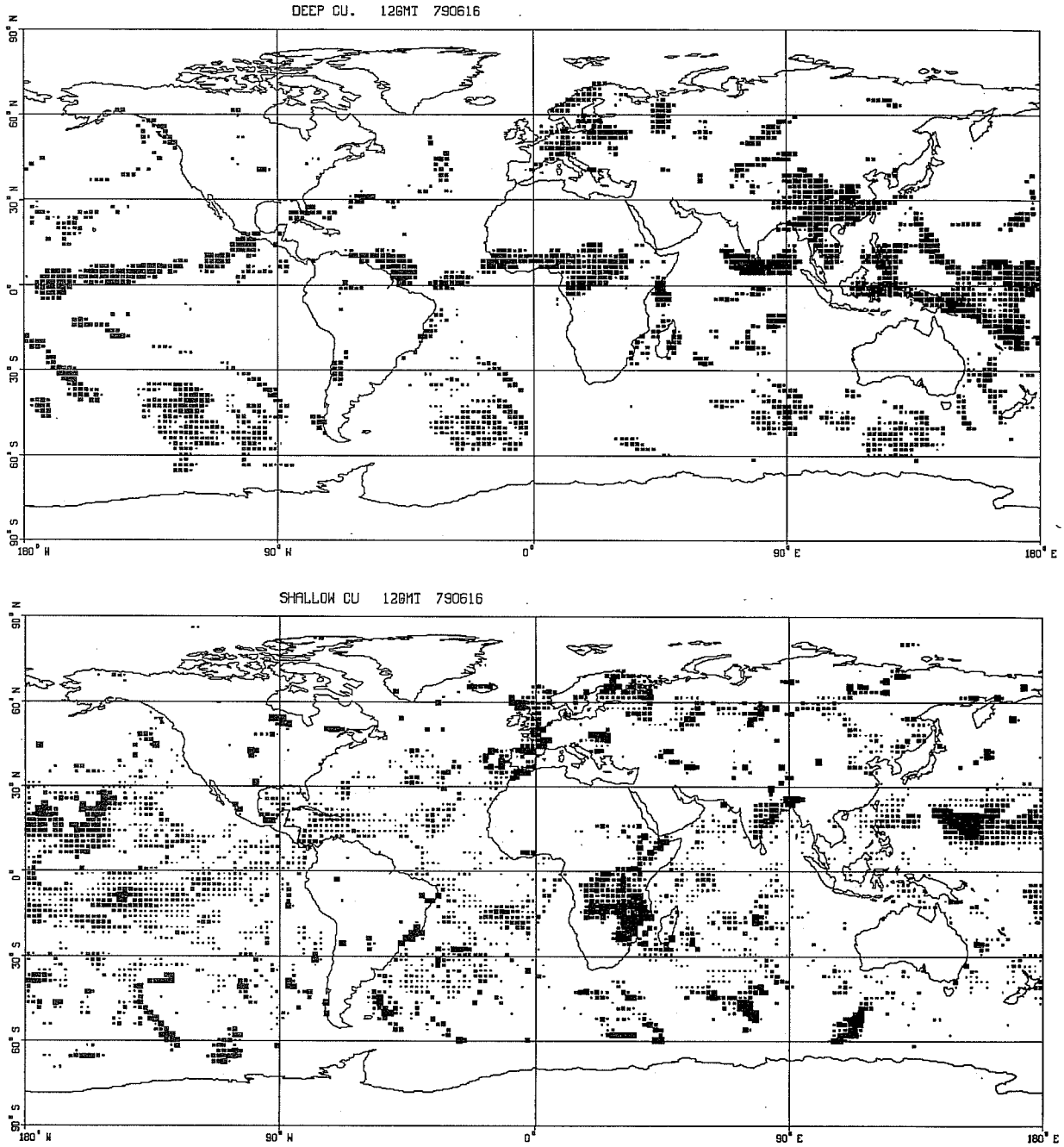

Fig. 11 Forecast maps of the 5-day predicted cloud cover
a) for shallow and deep convection
b) for total convective cloud and high cloud
c) METEOSAT Infra-red photograph for the same time

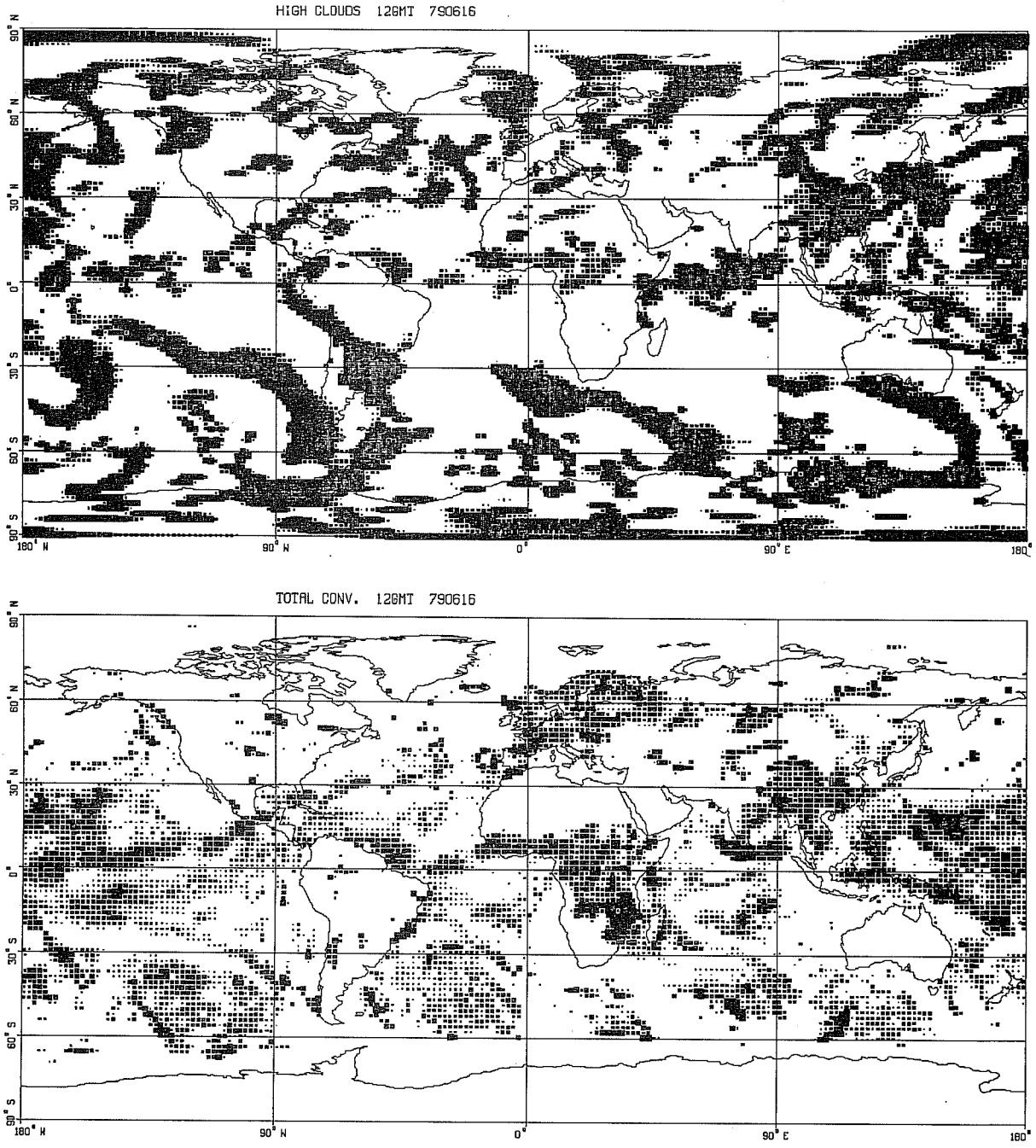

Fig. 11 b) For total convective cloud and high cloud

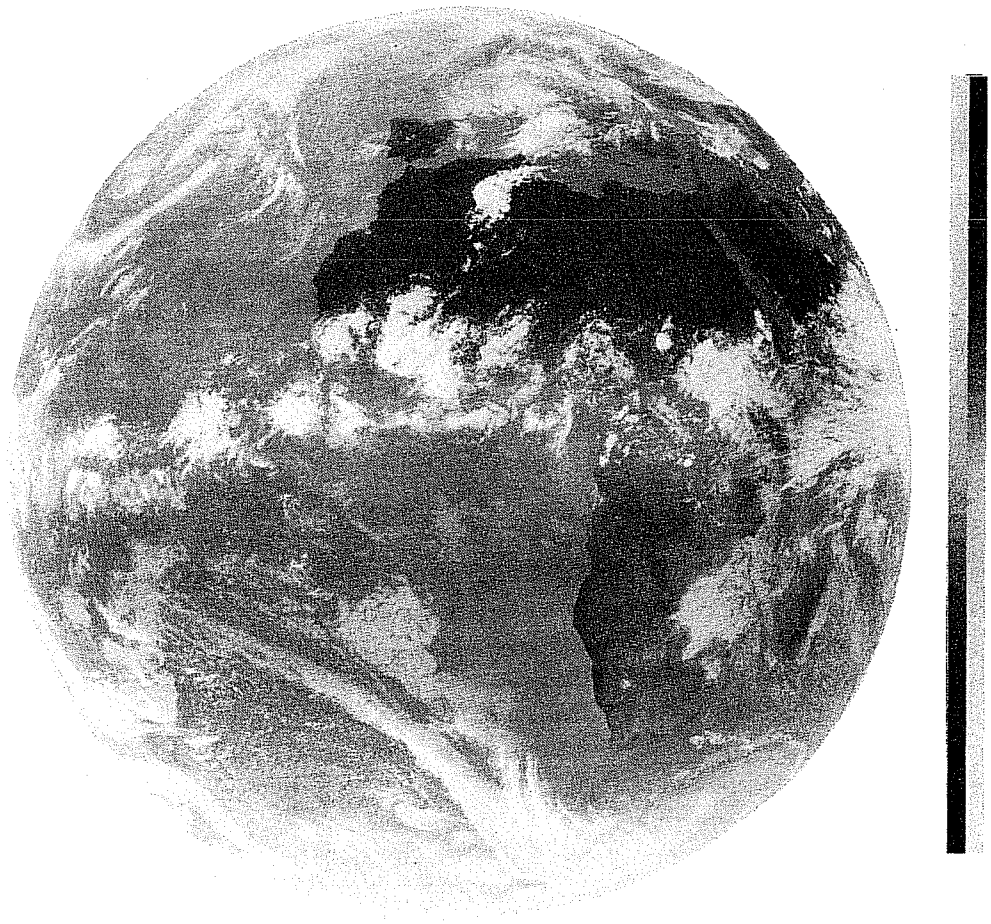

Fig. 11 c) METEOSAT Infra-red photograph for the same time

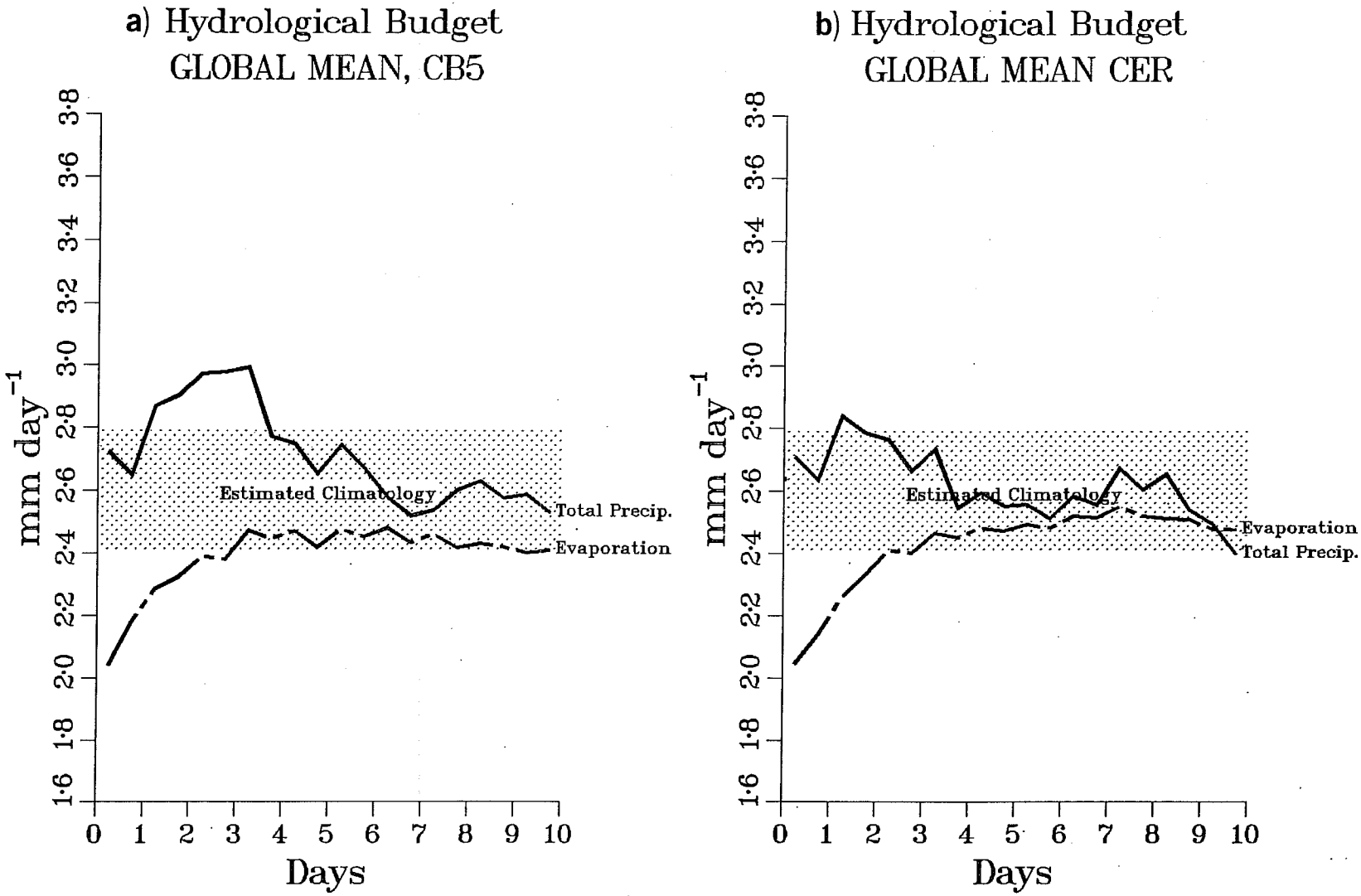

Fig. 12 Global rainfall and evaporation rates for a) Control experiment b) Adjustment scheme for a T63 10 day forecast run from 11/06/79. Both initial analyses were consistent with the convection scheme used.

Fig. 10 and 11 show forecasts of precipitation and cloud cover type with some verification. The predicted 24-48 hr accumulated rainfall with the new scheme compares favourably with the data particularly with regard to areas of spurious light convective rainfall over land. The cloud cover pictures are included to show the typical partition of the convection between deep and shallow, and even for this day 5 forecast the associated METEOSAT image supports the general distribution well.

Convection plays an important role in the so-called spin-up period during which the physical and dynamical processes interact to generate small-scale motions not represented in the analysis and to re-establish adiabatic and diabatic balances which are difficult to properly achieve in the analysis. With the present model, this spin-up is a problem as shown in Fig. 12a. Model resolution and diffusion parameters significantly affect this behaviour, nevertheless, it appears that the adjustment scheme may alleviate this problem to some extent, Fig. 12b.

5.2 50-day integration

Figs. 13-15 show mean fields for a 50-day T63 integration with the adjustment scheme (ADJ) starting from the analysis for 15 June 1984 and a corresponding control integration with operational physics (CTRL). The forecast means are for the last 30 days of the integration and the analysed mean flow (ANAL) is from the Centre's analyses for July 1984.

(a) Precipitation

Fig. 13 compares the two forecast mean precipitation maps with the July climatology published by Jaeger (1976). Obviously there can be large interannual variability in precipitation (and cloudiness), nevertheless the figures still make interesting comparison reflecting the large-scale flow

differences and also differences in the physics directly. While concentrating on differences, it is clear that both simulations reproduce the main climatological features. Both integrations show a well-marked ITCZ with a more marked Atlantic ITCZ for ADJ and a more marked Pacific ITCZ in CTRL. The most marked differences are in the Asian monsoon region and the Western Pacific. While both show the monsoon maxima, the intensities and location are different and, together with the enhanced precipitation region in ADJ over the West Pacific, indicate a substantially different divergent flow field in this area as discussed later.

In the area 40°E-60°E in low latitudes the very marked break in the rainfall is well simulated by ADJ. The previously noted problem concerning operational overprediction of light convective rain is emphasised when comparing the low rainfall regions such as those south of the equator in the Pacific, Atlantic and Indian oceans; a recent modification to the Kuo scheme may have alleviated this problem to some extent. Mean cloud cover maps (not shown) reflect the above precipitation differences since the cloud cover and precipitation schemes are strongly linked.

(b) The mean flow

Figs. 14 and 15 show the 200 mb and 850 mb mean flow and it is clear that the general structure of the tropospheric flow is very well simulated despite the difficulties of time-averaging the transient waves over a 30-day period. In general, the new convection scheme's simulation has better structure at both 200 and 850 mb. Notable features at 200 mb are the ridge in the vicinity of the Caspian Sea and the circulation over the west Pacific including the marked weakening of the tropical easterlies. Linked to the Caspian ridge is an improved flow in the European sector. However, the flow in the vicinity of North America is rather less well simulated. At 850 mb the monsoon

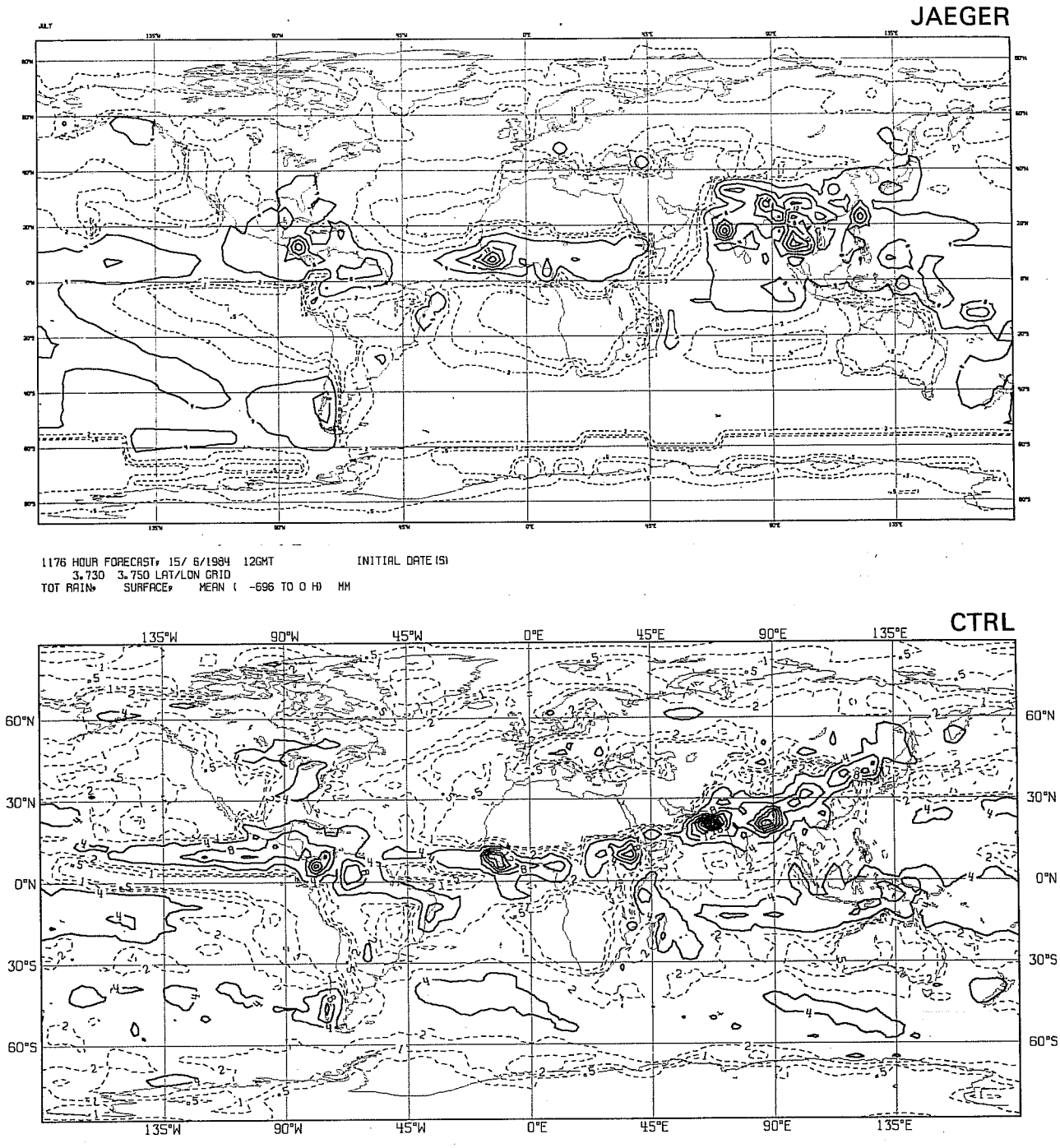

Fig. 13 The mean rainfall for the last 30 days of 50 day T63 forecasts from 15/6/84 compared with a July climatology (Jaeger, 1976).

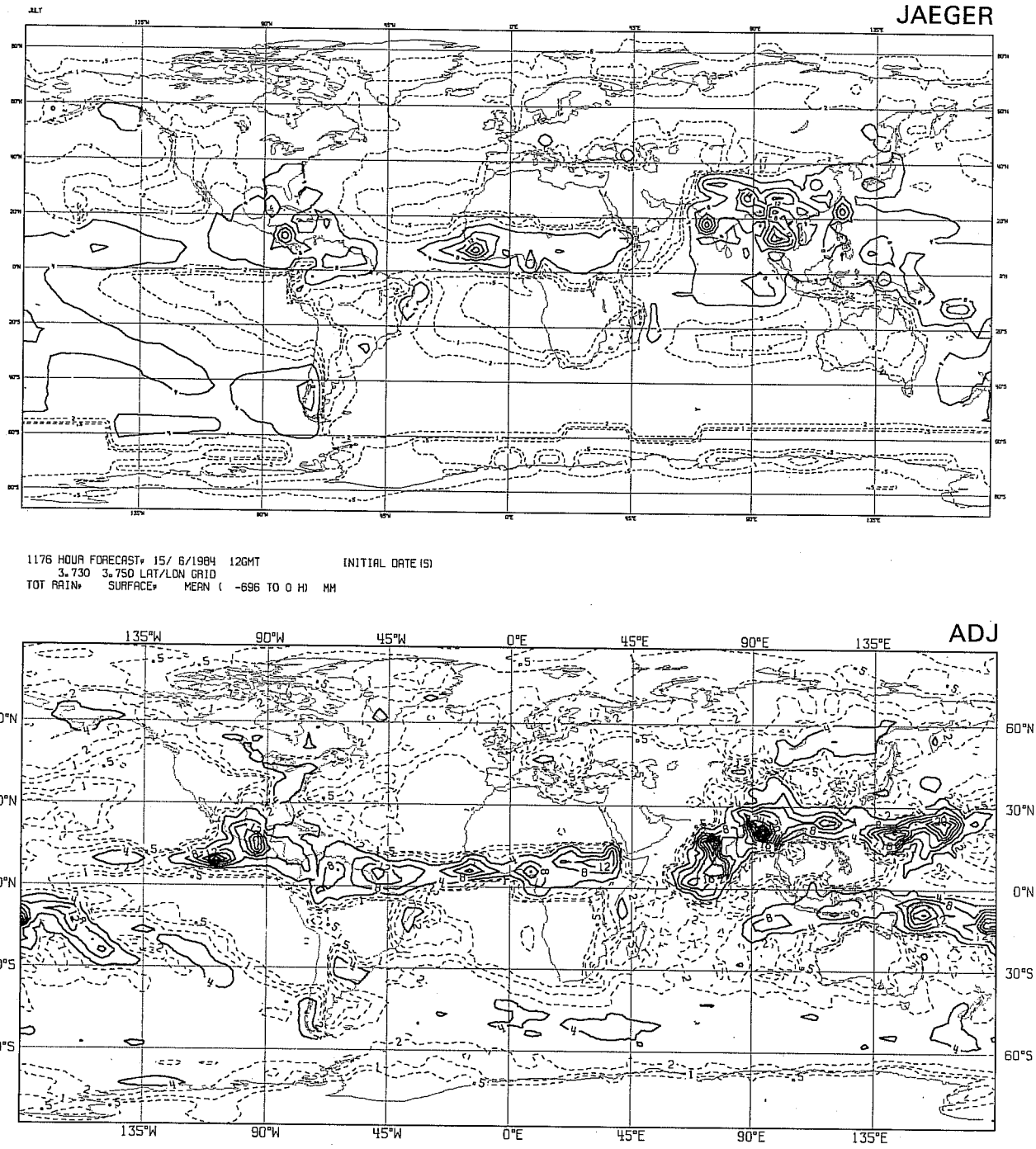

Fig. 13 continued

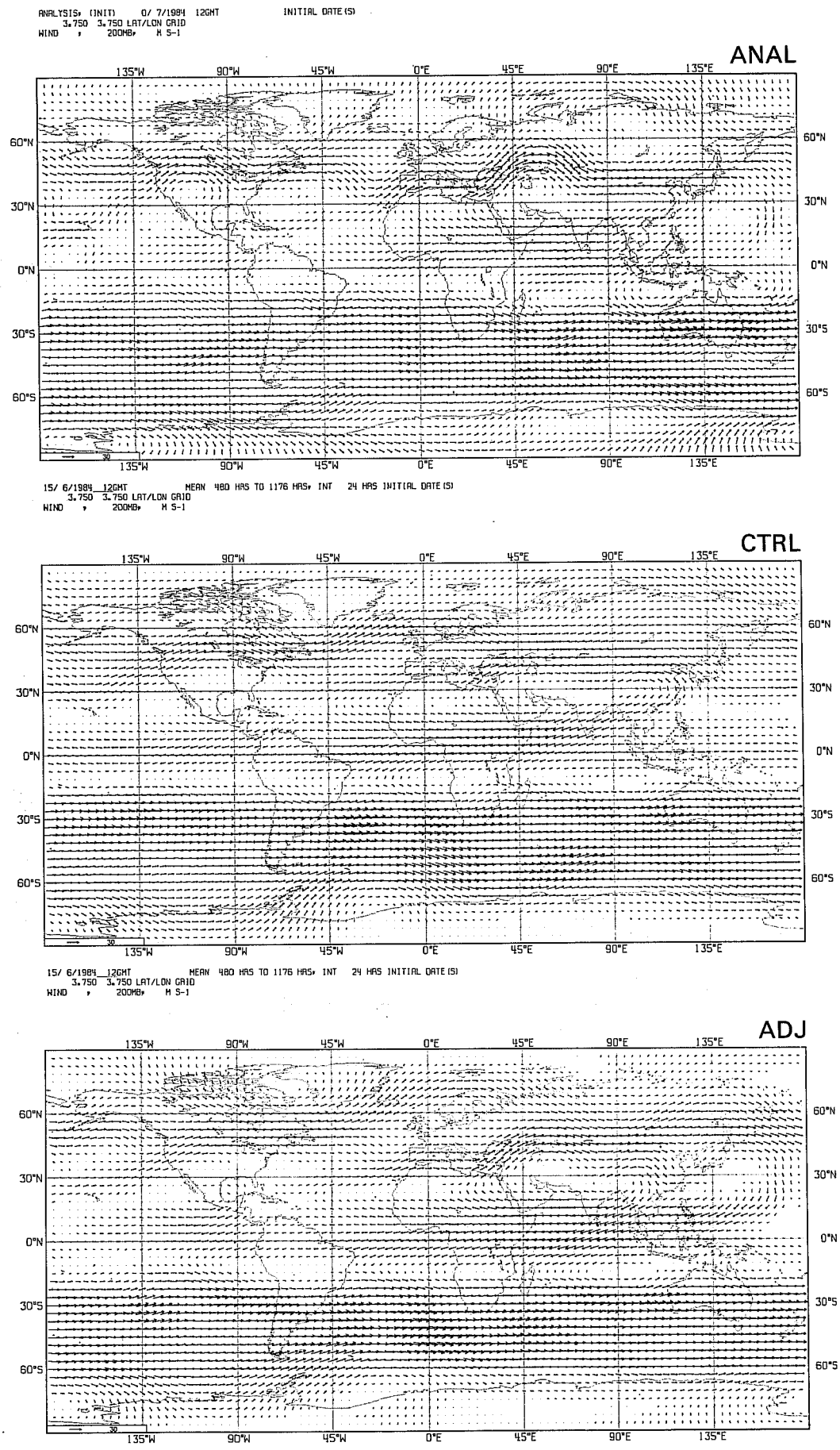

Fig. 14 As Fig. 13 but for the 200 mb wind compared with the July 1984 mean analysis.

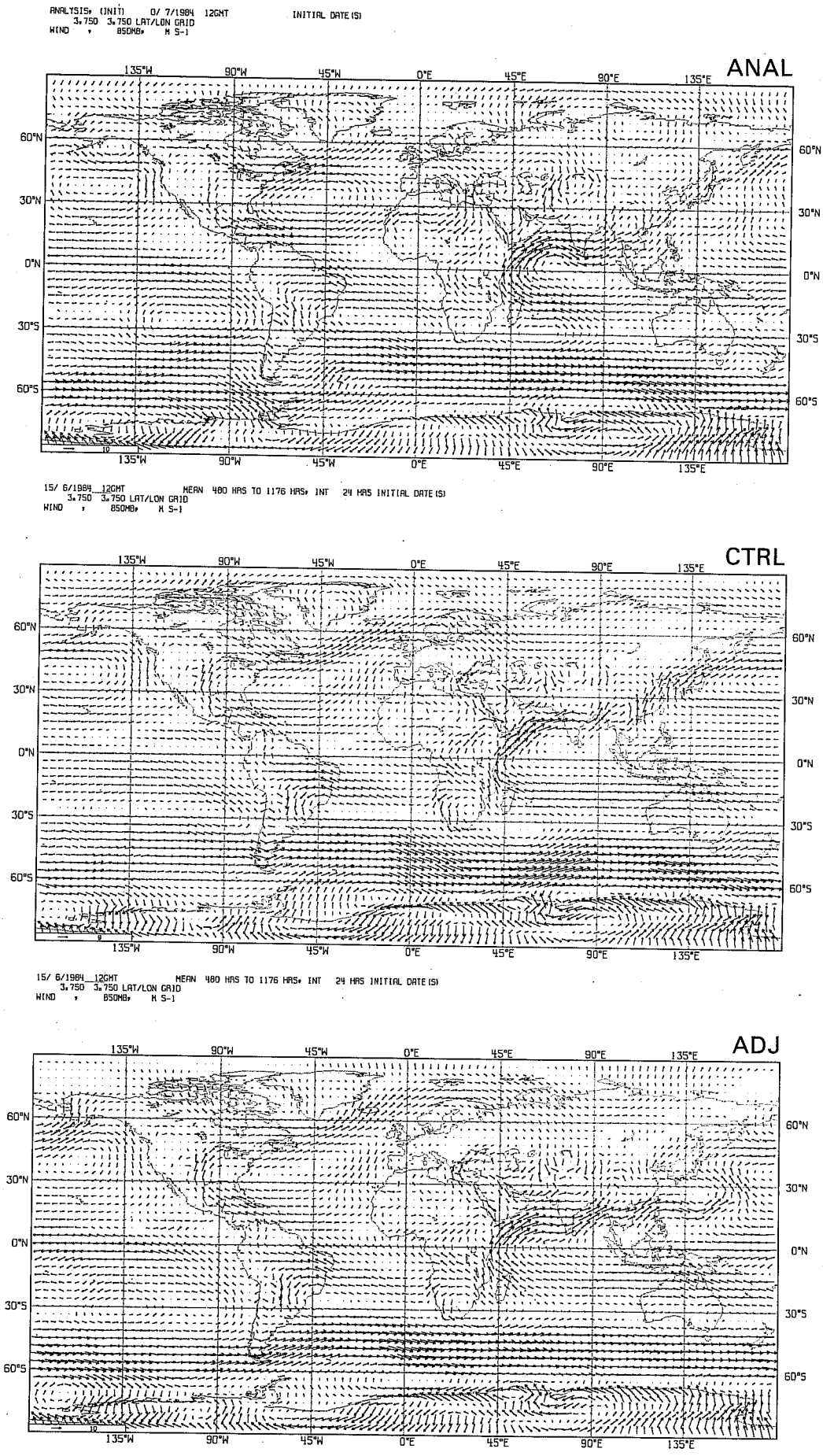

Fig. 15 As Fig. 14, for 850 mb.

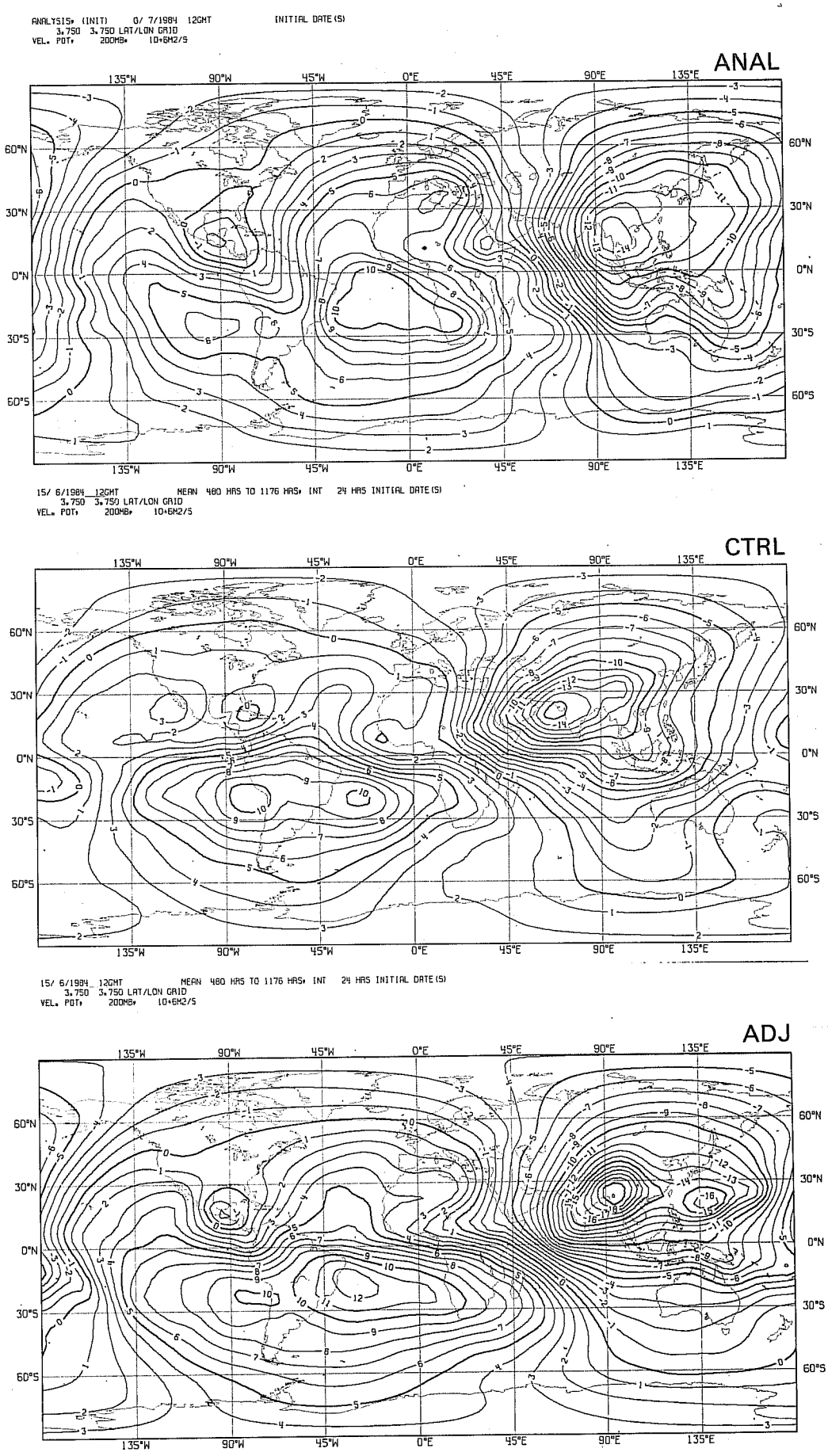

Fig. 16 As Fig. 14 for the 200 mb velocity potential.

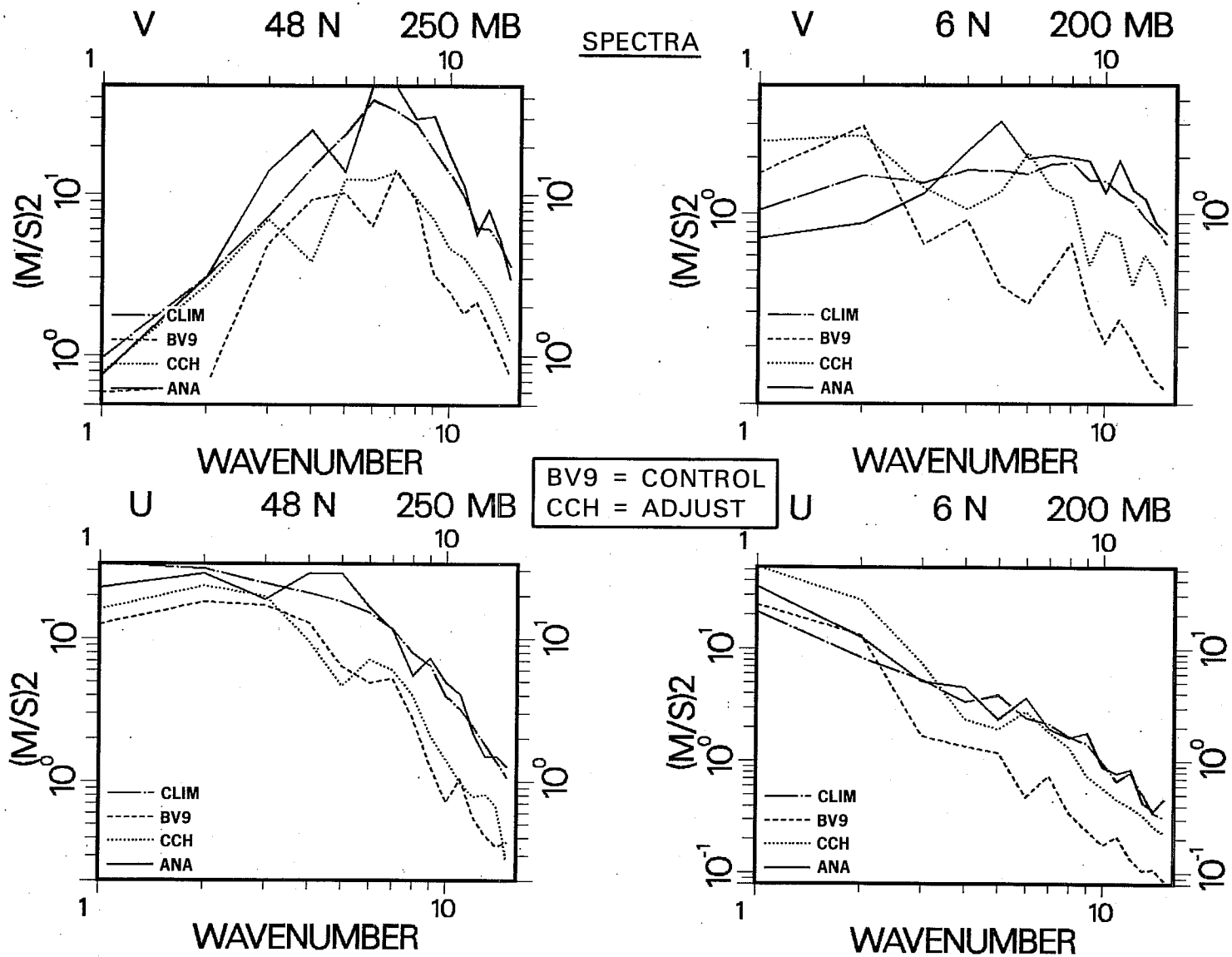

Fig. 17 Mean wind spectra for days 20-50 for two latitude/pressure values compared with analysis and climatology.

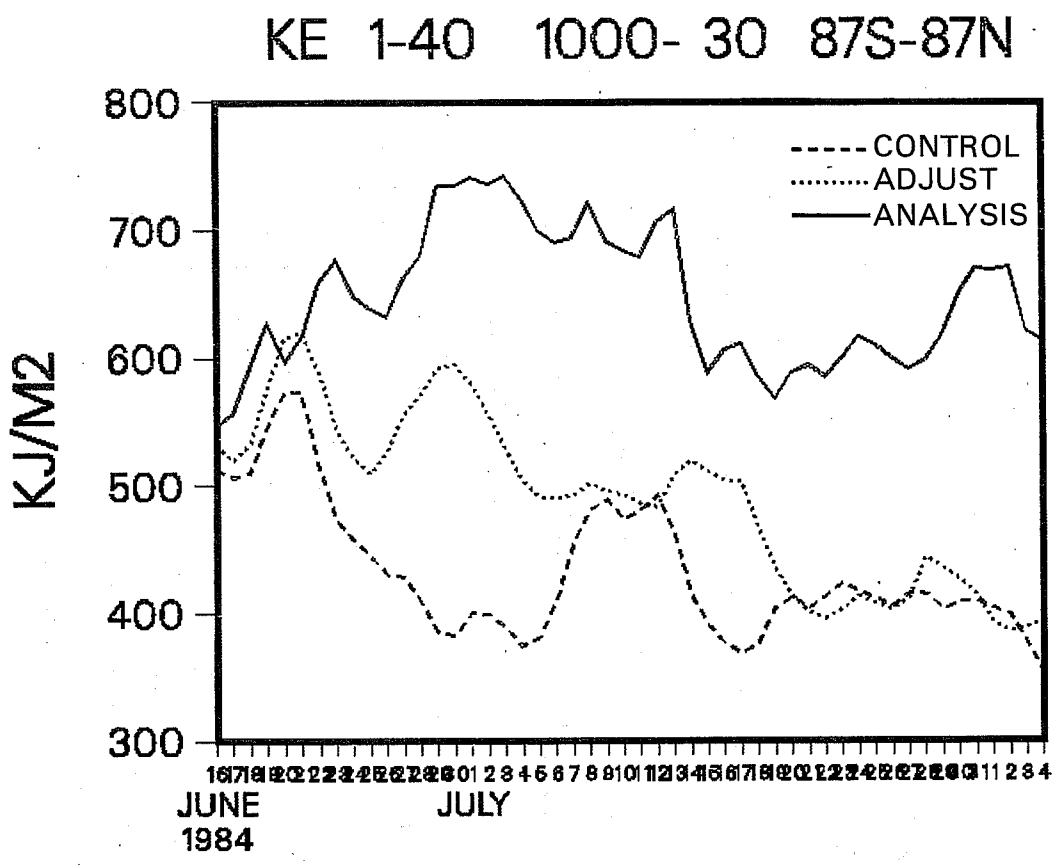

Fig. 18 The evolution of the global-mean eddy kinetic energy during the 50 day forecasts compared with the analyses.

circulation over the Indian ocean and its extension through to the Pacific is well simulated in ADJ, and both simulations capture the 'monsoon-like' flow into the south part of the USA.

Fig. 16 shows the mean velocity potential at 200 mb describing the divergent part of the flow. Comparison of the simulations with the analyses shows significant differences which favour the new convection scheme, although noticeable errors still remain, particularly over the Pacific. The main outflow region over south east Asia is better located but possibly too intense and the secondary outflow region over the Caribbean is better developed and located.

(c) Other diagnostics

This discussion of an extended integration is not intended to be exhaustive and only a small subset of results have been shown. Global diagnostics in terms of energetics and spectral analysis can be illuminating, and Fig. 17 and Fig. 18 show examples of time-mean spectra and eddy kinetic energy. Fig. 17 shows distinct improvements in the midlatitude spectrum of the meridional wind and of the tropical wind spectra. A particularly interesting result is shown in Fig. 18, in which the globally averaged eddy kinetic energy values are plotted as a function of time. The maintaining of eddy kinetic energy levels well beyond ten days of the forecast with the new scheme emphasises the importance of improved convective parameterization in the longer-term integrations.

6. CONCLUDING REMARKS

Experience with the new convective adjustment scheme as exemplified by the results presented here is very encouraging, and suggests that the approach is particularly beneficial for medium and extended-range forecasts. Bearing in mind that the new scheme is still in its infancy (c.f. Kuo, Arakawa-Schubert), it appears that this scheme is a viable alternative to existing operational and research parameterizations, and that future development and sophistication will improve matters further. Use of the new scheme in climate and higher resolution models has not yet been tried.

For climate simulations the basic premise of the new scheme seems sound and should not suffer from some of the biases that existing schemes exhibit. For mesoscale/high resolution limited area modelling, the fact that the new scheme is very smooth in time and computational well-behaved may benefit this scale of modelling. Recent experiences indicate that a shortening of the adjustment timescale is necessary as the local forcing is better resolved.

Several improvements and extensions to this work are in progress, and in particular, recent developments in the understanding of convection in baroclinic regions (Emanuel, 1979, 1982, 1983a,b; Thorpe, 1983; Thorpe and Emanuel, 1985) enable a straightforward extension of the scheme to parameterize this "slantwise" convection.

The new scheme is a thermodynamic adjustment and there is no basis for parameterizing the momentum or vorticity transports by deep convection in such a way. However, by linking the new scheme to the dynamical parameterization scheme developed by Miller and Moncrieff (1983) it should be possible to parameterize momentum transports in a reasonably consistent way.

Acknowledgements

Much of the formulation, development and testing was done together with Dr. Alan Betts, whose ideas form the basis of the scheme. For the substantial efforts and ingenuity required to incorporate the original scheme into the ECMWF model, I thank Bodo Ritter who turned "water into wine"! Thanks are also due to several Research Department staff who provided some of the figures.

References

Arakawa, A. and W.H. Schubert, 1974: Interaction of a cumulus cloud ensemble with the large-scale environment: Part I. J.Atmos.Sci., 31, 674-701.

Augstein, E., H. Riehl, F. Ostopoff, and V. Wagner 1973: Mass and energy transports in an undisturbed Atlantic trade-wind flow. Mon.Wea.Rev., 101, 101-111.

Betts, A.K. 1973: Non-precipitating cumulus convection and its parameterization. Quart.J.Roy.Meteor.Soc., 99, 178-196.

Betts, A.K. 1984: Atmospheric convective structure and a convection scheme based on saturation point methods. ECMWF Workshop on Convection in Large-Scale Numerical Models, 28 November - 1 December, 1983, Reading, U.K., 69-94.

Betts, A.K. and M.J. Miller, 1984: A new convective adjustment scheme. ECMWF Tech.Rep.No.43, 68 pp.

Emanuel, K.A., 1979: Inertial instability and mesoscale convective systems. Part I: Linear theory of inertial instability in rotating viscous fluids. J.Atmos.Sci., 36, 2425-2449.

Emanuel, K.A., 1982: Inertial instability and mesoscale convective systems. Part II: Symmetric CISK in a baroclinic flow. J.Atmos.Sci., 39 1080-1097.

Emanuel, K.A., 1983(a): The Lagrangian parcel dynamics of moist symmetric instability J.Atmos.Sci., 40, 2368-2376.

Emanuel, K.A., 1983(b): On assessing local conditional symmetric instability from atmospheric soundings. Mon.Wea.Rev., 111, 2016-2033.

Holland, J.Z., and E.M. Rasmusson, 1973: Measurements of the atmospheric mass, energy and momentum budgets over a 500 km square of tropical ocean. Mon.Wea.Rev., 101, 44-55.

Jaeger, L., 1976: Monatskarten des Niederschlages für die ganze Erde. Ber.Dtsch.Wetterd., Offenbach/Main, No. 139, Vol. 19, 38 pp.

Kuo, H.L., 1965: On formation and intensification of tropical cyclones through latent heat release by cumulus convection. J.Atmos.Sci., 22, 40-63.

Kuo, H.L., 1974: Further studies of the parameterization of the influence of cumulus convection on large-scale flow. J.Atmos.Sci., 31, 1232-1240.

Lord, S.J., 1982: Interaction of a cumulus cloud ensemble with the large-scale environment Part III: Semi-prognostic test of the Arakawa-Schubert cumulus parameterization. J.Atmos.Sci., 39, 88-103.

Lord, S.L., and A. Arakawa, 1980: Interaction of a cumulus ensemble with the large-scale environment. Part II. J.Atmos.Sci., 37, 2677-2692.

Ludlam, F.H., 1980: Clouds and Storms. Pennsylvania State Univ., 407pp plus plates.

Miller, M.J., and M.W. Moncrieff, 1984: The use and implementation of dynamical cloud models in a parameterisation scheme for deep convection. ECMWF Workshop on Convection in Large-Scale Numerical Models, 28 November - 1 December 1983, Reading, U.K., 33-67.

Økland, H., 1976: An example of air-mass transformation in the Arctic and connected disturbances of the wind field. Report DM-20, Univ. of Stockholm., 30pp.

Thompson Jr., R.M., S.W. Payne, E.E. Reckel and R.J. Reed, 1979: Structure and properties of synoptic-scale wave disturbances in the intertropical convergence zone of the eastern Atlantic. J.Atmos.Sci., 36, 53-72.

Tiedtke, M., 1982: Assessment of the PBL flow in the EC-model. ECMWF Workshop on Planetary Boundary Layer Parameterisation, 25-27 November 1981, Reading, U.K., 155-192.

Tiedtke, M., 1984: The sensitivity of the time-mean large-scale flow to cumulus convection in the ECMWF model. ECMWF Workshop on Convection in Large-Scale Numerical Models, 28 November - 1 December, 1983, Reading, U.K., 297-316.

Wagner, V., 1975: Relationships between the tropospheric circulation and energetic processes within the Hadley circulation over the Atlantic Ocean. Berichte Inst. Radiometeor. und Maritime Meteor. Univ. Hamburg, No26, 83pp.